FEBS Letters 555 (2003) 638–642 FEBS 27910

The intestinal zonula occludens toxin (ZOT) receptor recognises non-native ZOT conformers and localises to the intercellular contacts

Alvin Lee[a], Natalie White[b], Christopher F. van der Walle[a,*]

[a] *Pharmaceutical Sciences, Institute for Biomedical Sciences, University of Strathclyde, 27 Taylor Street, Glasgow G4 0NR, UK*
[b] *Department of Pharmacy and Pharmacology, University of Bath, Claverton Down, Bath BA2 7AY, UK*

Received 15 October 2003; revised 31 October 2003; accepted 13 November 2003

First published online 25 November 2003

Edited by Thomas L. James

Abstract A preliminary structural analysis of *Vibrio cholerae* zonula occludens toxin (ZOT) was made by equilibrium denaturation and circular dichroism. ZOT is a structurally unstable protein in aqueous solution ($\Delta G_{(H2O)}$ 3.82 kcal/mol), the putative intra- and extracellular domains unfold co-operatively, with complete denaturation via observed conformational intermediates. Refolding of denatured ZOT is not dependent on disulphide bridge formation. Partial refolding of a maltose binding protein–ZOT fusion did not prevent its specific binding to the ZOT receptor on Caco-2 cells. Immuno-gold labelling showed that the ZOT receptor localises to the intercellular contacts between cells in a confluent monolayer.

Key words: Zonula occludens toxin; Tight junction; Immunogold labelling; Protein unfolding; *Vibrio cholerae*

1. Introduction

Interest generated around *Vibrio cholerae* zonula occludens toxin (ZOT) can largely be attributed to its unusual transient loosening of the intestinal tight junctions (zonula occludens), rather than an irreversible opening as seen with *Clostridium difficile* toxin A [1]. The tight junctions regulate the permeability of solutes across the polarised epithelial cells at the mucosal surface and by scanning electron microscopy (SEM) are seen as a belt circumventing the cell at its apical side [2]. Existing as membrane microdomains, these structures are mainly composed of the occludin and claudin family of transmembrane proteins and the zonula occludens-associated proteins (ZO-1, 2, 3) [3–6].

Using in vivo perfusion assays, a 10-fold increase in insulin permeability across the rabbit jejunal and ileal mucosa, but not the colonic mucosa, was observed in response to ZOT [7]. The absence of a colonic response was seen as important because compromising the integrity of the lower bowel would facilitate pathogen infiltration. ZOT causes tight junction disruption between confluent Caco-2 monolayers in culture (although derived from an adenocarcinoma of the colon the cells phenotypically differentiate to enterocytes – small intestinal cells), seen as a transient 60% drop in transepithelial electrical resistance and increased permeation for certain drugs [8].

The mechanism by which ZOT elicits tight junction disruption is understood for the most part at the cellular level and partially at the molecular level. Micrographs of rabbit ileum exposed to culture supernatants of *V. cholerae* showed loss of strands perpendicular to the ZO axis, with the 10–30 kDa size fraction reversibly increasing tissue conductance [1]. Later work correlated the 10–30 kDa fraction to the ZOT C-terminus [9], and screening overlapping C- and N-terminally truncated ZOT constructs isolated a putative binding motif G^{291}RLCVQDG^{298}, within the 135 residue C-terminal active domain termed ΔG [10].

Western blot of protein preparations from intestine, heart and brain for anti-ZOT antibody identified a 47 kDa band, later termed zonulin, with N-terminal identity to GRLCVQDG^{298} and a similar action on the intestinal epithelium as ZOT [11]. A synthetic peptide analogue (GGVLVQPG) to the ZOT and zonulin putative binding motifs was shown to partially inhibit the intestinal response to ZOT and zonulin [10]. This octapeptide would not maintain any specific secondary structure but still inhibited ZOT binding to its putative receptor, showing that the GRLCVQDG^{298} putative binding domain of ZOT is not entirely conformationally constrained. Further information regarding the structural mechanism of action ideally requires cloning and expression of the putative ZOT receptor, which thus far has been isolated as a 66 kDa protein from Caco-2 cells and a 45 kDa protein from human brain, heart and intestine [12,13].

Conformational analysis of ZOT has to date not been available, though its intracellular signalling requires protein kinase C, and possibly phospholipase C, reducing the number of transcellular actin filaments with concomitant reciprocal changes to the F- and G-actin pools [14]. In this report we intend to address the above issues by preliminary characterisation of ZOT conformational stability with respect to receptor binding, and provide data which may aid further investigations targeting the isolation of the putative ZOT receptor.

2. Materials and methods

2.1. Cloning procedures

Genomic DNA was prepared from *V. cholera* TRH7000, an attenuated strain kindly provided by Prof. Hirst, University of Bristol [15]. This strain was constructed by deletion of both *ctxA*/*B* genes as previously described [16], that is: recombination of *V. cholerae* N16961 with a plasmid (pJBK55) harbouring a 20 kb chromosomal fragment of *V. cholerae* but with a β-lactamase gene substituted for the *ctxAB* genes. Since deletion of the *ctxAB* genes was made by *Acc*I digestion, where one of the three *Acc*I sites flanks the *ctxA* gene, a ~280 bp cassette was removed from the 3′-end of the *zot* gene. This 'missing' cassette was reconstructed using recursive polymerase chain

*Corresponding author. Fax: (44)-141-552 6443.
E-mail address: chris.walle@strath.ac.uk (C.F. van der Walle).

0014-5793/03/$22.00 © 2003 Published by Elsevier B.V. on behalf of the Federation of European Biochemical Societies.
doi:10.1016/S0014-5793(03)01348-6

reaction (PCR) [17], with the following primers (all 5′ to 3′): TAGAAGCTTCAATTTGGACATTCCTTATCGTGGTCTATGGGCGACAGGTCATCACATCTACAAG, GGACGCTGCCACTCTCGGTTTCAAAGAACACTGTAAGCGTATCCTTGTAGATGTGATGACCTG, CGAGAGTGGCAGCGTCCCAACAGAGCTGTTTGCCTCGAGCTACCGCTACAAGGTGCTACCGTT, GCGCTGCAAAGGTATCGAACACCACAAAGTGATTGAAATCCGGTAACGGTAGCACCTTGTAGC, TTCGATACCTTTGCAGCGCAAGCGCTGTGGGTAGAAGTGAAACGTGGTTTACCGATAAAGACAG, CTAGGTACCTTAAAATATACTATTTAGTCCTTTTTTATCATTTTCTGTCTTTATCGGTAAACCA. The 3′-truncated *zot* gene was amplified from the genomic DNA using the primers GAGGATCCATCTTTATTCATCACGGCGCG (fwd) and TAGAAGCTTAGGCGATAACGCTCATCAC (rev), digested with *Bam*HI and *Hin*dIII and ligated into similarly digested pBluescript II KS (Stratagene). This construct was then digested with *Hin*dIII and *Kpn*I so that the similarly digested 286 bp recursive PCR cassette could be ligated in frame in order to afford the full-length *zot* gene. The *Hin*dIII site was mutated back to the original *zot* sequence using the Quikchange protocol (Stratagene) and the *zot* cassette subcloned into pQE-80L (His-tag, Qiagen), at *Bam*HI and *Kpn*I sites, and then pMal-c2x (MBP fusion, NEB), at *Bam*HI and *Hin*dIII sites. DNA sequences of all plasmid constructs were verified on a PE ABI 377 DNA Sequencer using dRhodamine Dye Terminator chemistry.

2.2. *ZOT expression in* Escherichia coli

The *E. coli* strains DH5α, BLR and AD494 (Novagen) were screened for expression of ZOT from the pQE-80L/zot and pMal-c2x/zot constructs, grown at either 30°C or 37°C in Lennox broth containing 100 μg/ml ampicillin. The DH5α strain, grown at 37°C, was considered the most suitable. Cells were grown to an OD_{600} of 0.6, expression induced by addition of 0.1 mM isopropyl-β-D-1-thiogalactopyranoside (IPTG) and harvested 3 h later (yield around 3 g/l). Titration of IPTG concentration versus ZOT expression showed that 0.1 mM was optimal.

2.3. *ZOT purification and refolding*

For expression of His-tagged ZOT, the cell pellet was lysed in 6 M guanidine–HCl (GuHCl) for 30 min, centrifuged at $80\,000\times g$ for 1 h and loaded directly onto a 15 ml Ni^{2+}-Sepharose column, washed and eluted with 40 mM and 250 mM imidazole, respectively. Fractions containing ZOT were pooled, ZOT precipitated in 90% ethanol on ice and redissolved in 6 M GuHCl, phosphate-buffered saline (PBS), pH 7.4. Removal of the 33 kDa N-terminal ZOT fragment was achieved by size exclusion on a Superdex 75 column run on an AKTA FPLC system (Amersham Biosciences), equilibrated in 4 M GuHCl, PBS.

For expression of maltose binding protein–ZOT (MBP-ZOT), the cell pellet was lysed by addition of lysozyme (1 mg/ml), 0.01% Triton X100 in PBS for 30 min at 4°C and centrifuged at $80\,000\times g$. MBP-ZOT was refolded from the solubilised inclusion body fraction (6 M GuHCl) by 100-fold dilution into Tris–HCl, 0.1% Triton X-100, 5% glycerol, pH 7.5, concentrated (Millipore YM10 membrane) and partially purified by size exclusion on a Superdex 200 column. Protein purity was assessed by Coomassie staining of gels run in a sodium dodecyl sulphate–polyacrylamide gel electrophoresis system (Miniprotean, Bio-Rad). Concentrations of His-tagged ZOT were determined at A_{280} with a calculated molar extinction coefficient (ε) of 59 720 M^{-1} cm^{-1}.

2.4. *Enzyme-linked immunosorbent assay (ELISA)*

Quantitative assessment of MBP-ZOT concentrations was made by ELISA, against a standard curve for MBP. 96-well flat-bottomed plates (Fisher) were coated with doubling dilutions of MBP-ZOT or MBP in PBS, washed and blocked with 5% bovine serum albumin (BSA) for 1 h at 37°C. Wells were washed, incubated for 2 h, at 37°C, with mouse anti-MBP antibody (1:2000 dilution in 1% BSA, PBS) (Sigma), washed, and incubated for 1 h, at room temperature, with rabbit anti-mouse IgG peroxidase-conjugated antibody (1:2500 dilution) (Sigma). Wells were washed and substrate added (Sigma Fast™ OPD tablet set) according to the manufacturer's instructions. A_{405} was measured with background antibody binding in the absence of ligand subtracted from the readings.

2.5. *Cell culture*

Caco-2 cells were obtained from the European collection of cell culture (ECACC) and used between passage numbers 30 and 35. Cells were grown in Eagle's minimum essential medium (Sigma) supplemented with 10% foetal calf serum (Invitrogen), 2 mM L-glutamine (Invitrogen), 1% non-essential amino acids (Invitrogen), and 100 U/ml penicillin and 100 μg/ml streptomycin (Invitrogen). Cells were grown in 75 cm^3 flasks and maintained at 37°C and 5% CO_2 in a humidified incubator.

2.6. *Immunogold labelling and SEM*

Caco-2 cells were grown on glass coverslips for 5–7 days until confluent, washed with PBS and incubated in 1 μg/ml MBP-ZOT for 30 min at 37°C. Cells were washed, prefixed in 4% paraformaldehyde for 20 min and washed with 0.3 M glycine in PBS for 20 min. Cells were blocked for 15 min in block buffer solution with normal goat serum (Aurion, The Netherlands), washed in 0.1% BSA-c (Aurion) and incubated with mouse anti-MBP (1:2000 dilution) for 1 h. Following washes with 0.1% BSA-c, cells were incubated with 1/500 dilution of anti-mouse IgG gold conjugate (10 nm; Sigma) for 1 h. Cells were fixed in 2.5% glutaraldehyde in 0.1 M sodium cacodylate (pH 7.2) for 30 min, and incubated in silver enhancing solution (Aurion) for 10 min in the dark. Following washes in 0.1 M sodium cacodylate, cells were fixed in osmium tetroxide and dehydrated in acetone. Cells were viewed in a JEOL JSM6310 SEM with secondary and backscatter electron imaging. Non-paired *t*-test was made for gold particles within and outside a band equivalent to 1 μm around the periphery of cells in contact (for 40 cells, 308 particles).

2.7. *Equilibrium chemical denaturation*

Experiments were performed for purified His-tagged ZOT in 1–6 M GuHCl, PBS. The molarity of the GuHCl solution was calculated by weight [18]. Protein samples ($A_{280}\approx 0.3$) were rapidly diluted 11-fold in GuHCl and allowed to equilibrate for 10 min at 25°C before measuring fluorescence emitted at 350 nm over a 10 s period, using an excitation wavelength of 278 nm on a PTI spectrofluorometer, at 25°C. $\Delta G_{(H2O)}$ was calculated by extrapolation to 0 M GuHCl, fitting the data to a two-state unfolding mechanism for the first transition step and extrapolating for lack of baseline fluorescence at low GuHCl concentrations [18,19].

2.8. *Circular dichroism (CD)*

Spectra were recorded on a JASCO J-600 spectropolarimeter for purified His-tagged ZOT in 2 M $GuHCl_{(aq)}$ at a concentration of ~0.77 mg/ml (A_{280} 1.0). CD measurements were made in quartz cells with a path length of 0.05 cm for studies conducted in the peptide region (200–250 nm) and 1.0 cm in the disulphide-aromatic region (240–360 nm). Baseline corrections of the raw data and conversion of ΔA to $\Delta\varepsilon$ were performed using a mean amino acid mass of 115.

3. Results

3.1. *Protein expression*

Purification of His-tagged ZOT by metal chelation yielded two bands, one at ~33 kDa and the other at ~45 kDa, the same profile as reported by Uzzau et al. [9] (Fig. 1). Size exclusion chromatography isolated the full-length His-tagged ZOT, which remained stable. Refolding of His-tagged ZOT in aqueous buffer to concentrations required for spectroscopic analysis was not possible below 1–2 M GuHCl. The possible role of disulphide formation (ZOT has four Cys residues) in the folding pathway was investigated via expression in *E. coli* thioredoxin reductase mutants (strain AD494) and refolding in mixed redox buffers (reduced:oxidised glutathione, 5:0.5 mM) but no improved expression or refolding was observed.

MBP-ZOT was similarly expressed in the inclusion body fraction but refolding into aqueous buffer was possible, probably facilitated by the MBP carrier. Since the refolded fusion protein showed no affinity for amylose-conjugated Sepharose resin it appears that soluble intermediates were formed during the refolding process. Again, no requirement for disulphide formation in refolding was evident using the same procedures

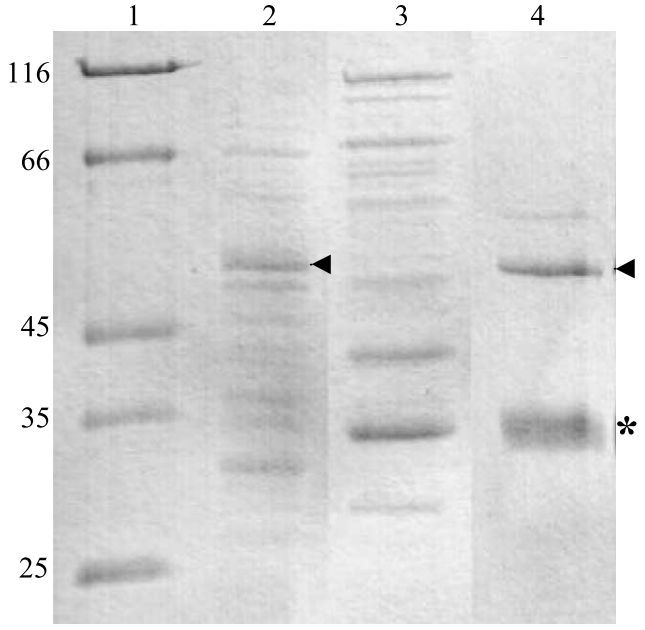

Fig. 1. Expression and purification of His-tagged ZOT. Lane 1: markers, kDa; lane 2: crude cell pellet; lane 3, wash; lane 4, elution. Arrow: His-tagged ZOT; star: 33 kDa N-terminal ZOT fragment.

as for His-tagged ZOT. Partial purification of MBP-ZOT via size exclusion to ~50% homogeneity by ELISA analysis was made.

3.2. Structural stability and conformational organisation of ZOT

His-tagged ZOT unfolding via GuHCl showed an increase in fluorescence, implying an overall burying of Trp residues (eight) in the native conformation (Fig. 2). For unfolded or folded conformers in a two-state model, the observed two-step transition is suggestive of two domains of differing conformational stability. However, this assumption does not always hold since known domain pairs may unfold co-operatively [19], and two or more transitions may represent unfolding via structural intermediates. For this reason we sought conformational characterisation of ZOT via CD and ab initio modelling using HMMSTR secondary structure prediction [20]. At a concentration of 2 M GuHCl, CD spectra in the peptide region (Fig. 3) are representative of a random coil implying at least partial unfolding over the entire sequence. Further, no secondary structure repeats characteristic of defined domains (such as immunoglobulin and C-type lectin domains seen for invasin and intimin) were predicted for ZOT using the HMMSTR algorithm. Therefore, the plateau in the protein unfolding curve most probably exists due to the presence of structural intermediates; higher GuHCl concentrations leading to complete unfolding. The His tag itself is not expected to contribute to changes in fluorescence since it is accepted that the tag is structurally non-defined and contains no Trp residues. $\Delta G_{(H2O)}$ for ZOT was calculated as 3.82 kcal/mol, corresponding to a protein of poor structural stability as may be expected from the refolding experiments [19] (Fig. 4). No contribution from disulphides or Trp was observed for CD spectra in the disulphide-aromatic region (data not shown), the absence of disulphides being consistent with the protein expression and refolding data.

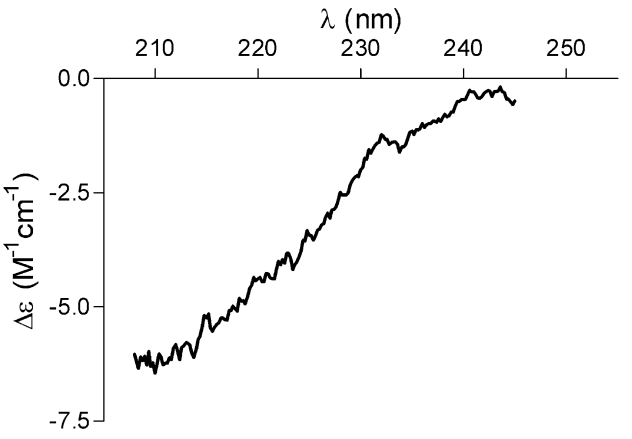

Fig. 3. CD spectra for His-tagged ZOT in 2 M $GuHCl_{(aq)}$, indicative of a random coil.

3.3. Localisation of the ZOT receptor

For backscatter images of cells incubated with MBP-ZOT, silver-coated gold particles were clearly observed as 'white dots', with X-ray analysis of the white dots showing peaks corresponding to silver. The images suggest that MBP-ZOT localised to the boundary between confluent Caco-2 cells (Fig. 5A,B), and a statistically significant difference ($P < 0.01$) was

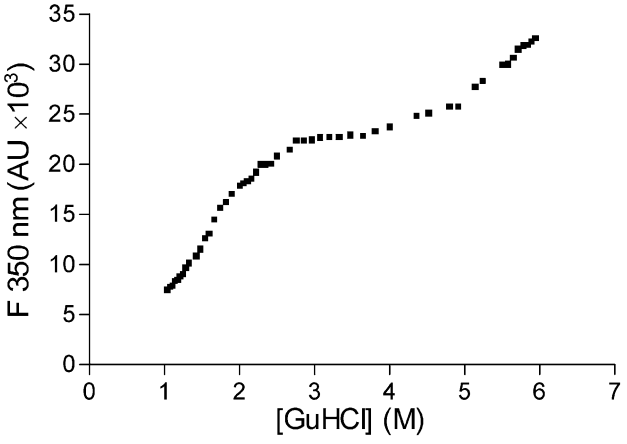

Fig. 2. GuHCl-induced denaturation of purified His-tagged ZOT, showing two transition regions.

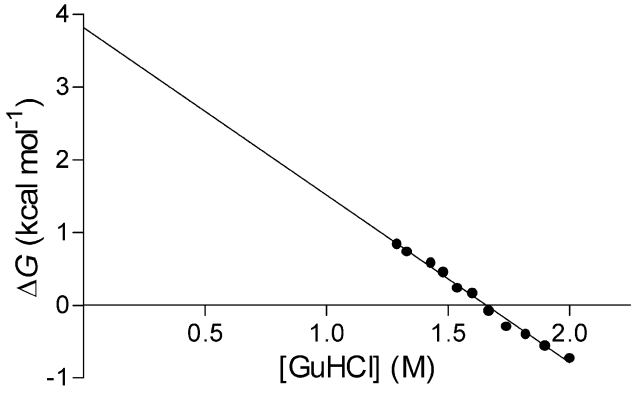

Fig. 4. Linear regression analysis for the calculation of $\Delta G_{(H2O)}$ for His-tagged ZOT for the first transition in the unfolding curve (slope, $m = 2.3$ kcal/mol M).

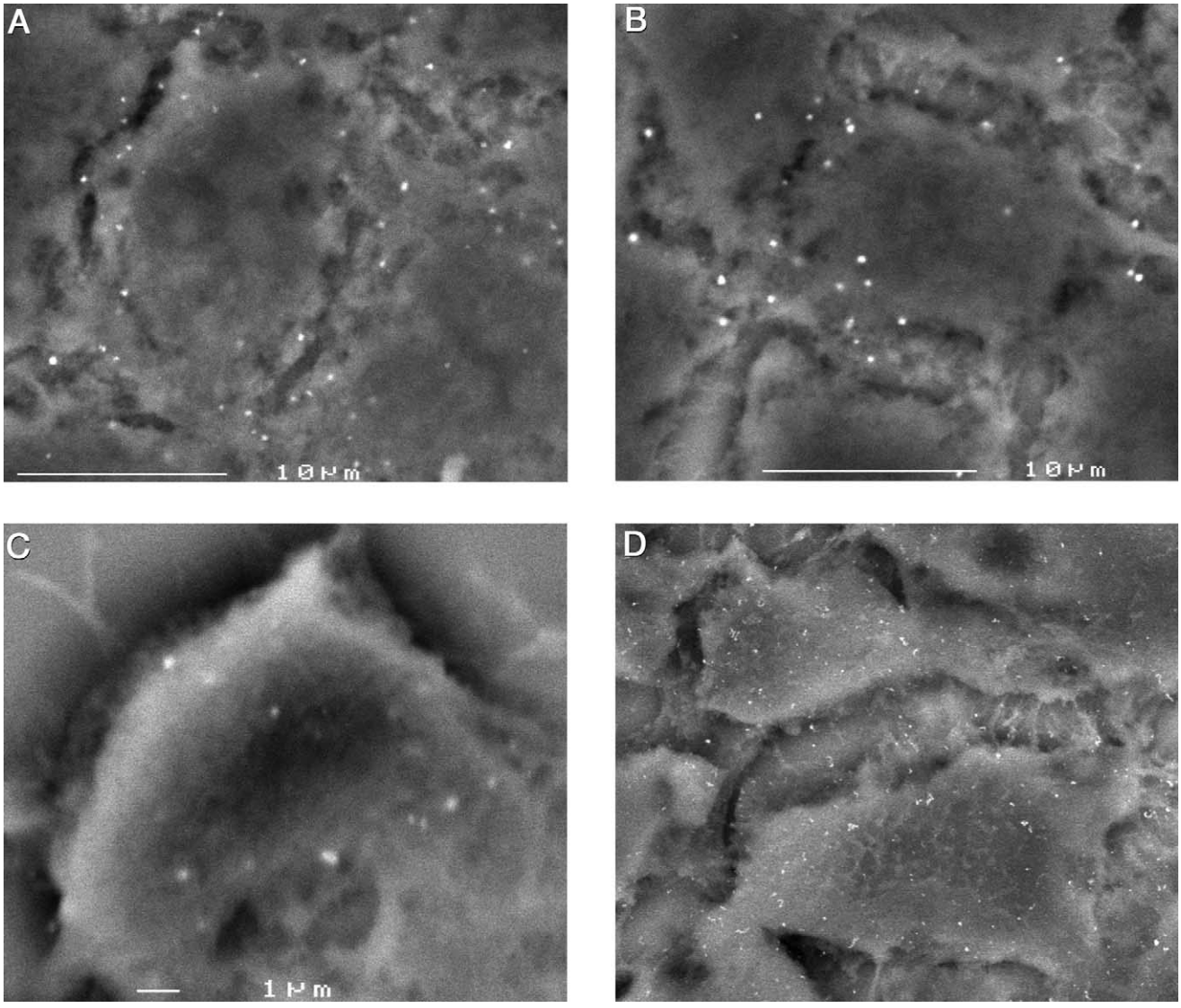

Fig. 5. SEM images of Caco-2 cells labelled for the ZOT receptor with gold colloid. A,B: Representative images of confluent cells incubated with MBP-ZOT. C: Isolated cell detaching from the surface incubated with MBP-ZOT. D: Cells incubated with MBP (control).

found between the means for the populations of gold particles within and outside a 1 μm region at the cell contacts (Fig. 6). MBP-ZOT was also seen to bind to isolated Caco-2 cells showing partial detachment from the surface (Fig. 5C), suggesting that processing of the ZOT receptor to the cell membrane is not dependent on cell attachment–polarisation. Too few partially detached cells prevented their statistical analysis for receptor localisation. Analysis of 20% and 50% confluent monolayers was attempted but isolated cells commonly detached during preparation for SEM and, since the cells grow in patches, intercellular contacts are as for the 100% confluent monolayer. MBP (control) showed no affinity for the cell surface (Fig. 5D); the 'white flecks' seen in these backscatter images are distinct from the white dots of gold colloid. X-ray analysis of these white flecks confirmed the absence of silver but presence of osmium.

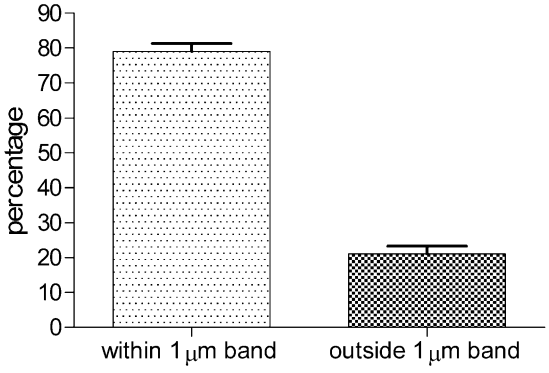

Fig. 6. Percentage of gold particles within and outside the 1 μm region for cell contact, error bars show S.E.M.

4. Discussion

A preliminary structural analysis of ZOT is provided, CD and protein unfolding data demonstrating that full-length ZOT is structurally unstable in solution, undergoing rapid unfolding in mild denaturant. Thus, it is not surprising that we have observed poor refolding characteristics for GuHCl-denatured His-tagged ZOT, especially since refolding of ZOT appears to proceed via intermediate conformers. The poor

conformational stability of ZOT isolated in aqueous solution is consistent with evidence that ZOT is a membrane-spanning protein [9], with hydropathy analysis of ZOT proposing a transmembrane segment over residues 220–235 [21]. The CD spectra and refolding data provide evidence that disulphide formation is not required for the proper folding of ZOT. This is consistent with the observation that two cysteines lie within the N-terminal fragment exposed to the reducing milieu of the bacterium [9], and Cys^{289}-Cys^{294} oxidation is highly unlikely given the unfavourable entropy change over the peptide backbone.

It is interesting to note that while refolding of MBP-ZOT did not yield a native conformation for MBP or ZOT, specific binding to the putative ZOT receptor on Caco-2 cells was still observed. This provides a structural basis for the observed partial inhibition of ZOT activity by an inherently flexible octapeptide, GGVLVQPG [10]. This scenario is similar to mimicry of the cell adhesion activity of fibronectin by the RGD tripeptide, for which the mechanism is now known to be a consequence of the RGD motif residing on a flexible loop protruding from the 10th type III fibronectin domain [22].

Finally, we show that the ZOT receptor is not merely randomly distributed at the cell surface, as would be sufficient to initiate actin depolymerisation, but localises to intercellular contacts. This suggests that the ZOT receptor may be associated with tight junction-associated proteins such as ZO-1, which would not be surprising given its action. However, our data are not entirely consistent with images of ZOT-conjugated fluorescent microspheres bound to cells, showing a more dispersed distribution [12]. The difference may be that these previously reported cell images are not indicative of a confluent monolayer and presents the possibility that the ZOT receptor migrates to the cell periphery during cell–cell contact. Uzzau et al. [12] also suggested that the ZOT receptor was internalised but unfortunately no *z*-axis image or statistical analysis of the cells were provided; our SEM images are not able to provide evidence for or against internalisation of the receptor. Further work needs to be directed to the potential interaction of the ZOT receptor with the tight junction-associated proteins, possibly via co-immunoprecipitation experiments, and how this is influenced by the binding of ZOT.

Acknowledgements: We are indebted to Dr Ursula Potter for SEM support and Dr Ian Jones for advice on the statistical analysis of the SEM images. This research was supported by the BBSRC, Grant E16523 to C.F.V.D.W.

References

[1] Fasano, A., Baudry, B., Pumplin, D.W., Wasserman, S.S., Tall, B.D., Ketley, J.M. and Kaper, J.B. (1991) Proc. Natl. Acad. Sci. USA 88, 5242–5246.
[2] Gumbiner, B. (1987) Am. J. Physiol. 253, C749–C758.
[3] Furuse, M., Hirase, T., Itoh, M., Nagafuchi, A., Yonemura, S. and Tsukita, S. (1993) J. Cell Biol. 123, 1777–1788.
[4] Furuse, M., Fujita, K., Hiiragi, T., Fujimoto, K. and Tsukita, S. (1998) J. Cell Biol. 141, 1539–1550.
[5] Gonzalez-Mariscal, L., Betanzos, A. and Avila-Flores, A. (2000) Semin. Cell Dev. Biol. 11, 315–324.
[6] Nusrat, A., Parkos, C.A., Verkade, P., Foley, C.S., Liang, T.W., Innis-Whitehouse, W., Eastburn, K.K. and Madara, J.L. (2000) J. Cell Sci. 113, 1771–1781.
[7] Fasano, A. and Uzzau, S. (1997) J. Clin. Invest. 99, 1158–1164.
[8] Cox, D.S., Raje, S., Gao, H., Salami, N.N. and Eddington, N.D. (2002) Pharm. Res. 19, 1680–1688.
[9] Uzzau, S., Cappuccinelli, P. and Fasano, A. (1999) Microb. Pathog. 27, 377–385.
[10] Di Pierro, M., Lu, R., Uzzau, S., Wang, W., Margaretten, K., Pazzani, C., Maimone, F. and Fasano, A. (2001) J. Biol. Chem. 276, 19160–19165.
[11] Wang, W., Uzzau, S., Goldblum, S.E. and Fasano, A. (2000) J. Cell Sci. 113, 4435–4440.
[12] Uzzau, S., Lu, R., Wang, W., Fiore, C. and Fasano, A. (2001) FEMS Microbiol. Lett. 194, 1–5.
[13] Lu, R., Wang, W., Uzzau, S., Vigorito, R., Zielke, H.R. and Fasano, A. (2000) J. Neurochem. 74, 320–326.
[14] Fasano, A. et al. (1995) J. Clin. Invest. 96, 710–720.
[15] Hirst, T.R., Sanchez, J., Kaper, J.B., Hardy, S.J. and Holmgren, J. (1984) Proc. Natl. Acad. Sci. USA 81, 7752–7756.
[16] Kaper, J.B., Lockman, H., Baldini, M.M. and Levine, M.M. (1984) Nature 308, 655–658.
[17] Prodromou, C. and Pearl, L.H. (1992) Protein Eng. 5, 827–829.
[18] Pace, C.N. and Scholtz, J.M. (1997) in: Protein Structure, A Practical Approach (Creighton, T.E., Ed.), pp. 299–321, IRL Press, Oxford.
[19] Van Der Walle, C.F., Altroff, H. and Mardon, H.J. (2002) Protein Eng. 15, 1021–1024.
[20] Bystroff, C., Thorsson, V. and Baker, D. (2000) J. Mol. Biol. 301, 173–190.
[21] Koonin, E.V. (1992) FEBS Lett. 312, 3–6.
[22] Copie, V. et al. (1998) J. Mol. Biol. 277, 663–682.